【カテゴリーII】

日本建築学会計画系論文集　第547号，17-25，2001年9月
J. Archit. Plann. Environ. Eng., AIJ, No. 547, 17-25, Sep., 2001

MEASUREMENT OF PROJECTED AREA FACTORS FOR THERMAL RADIATION ANALYSIS ON EACH PART OF THE HUMAN BODY

人体各部を対象とした放射解析のための投影面積率測定

Masayuki OGURO, Edward ARENS**, Hui ZHANG***,*
*Kazuyo TSUZUKI**** and Tadahisa KATAYAMA******
大黒雅之，エドワード アレンズ，ウイ チャン，都築和代，片山忠久

This paper provides projected area factors for each part of the human body to allow the radiative heat transfer between the human and surrounding surfaces to be calculated. We first describe ways of calculating angle factors, effective radiation area, radiative heat transfer coefficients, and the mean radiant temperature for each segment of the human body. Then we describe an approach to measuring projected area factors using a manikin. Projected area factor distributions and other important elements for radiation analysis are presented and compared with other studies.

Keywords : *Radiative heat transfer, projected area factors, human body, thermal comfort, asymmetric thermal environment*
放射熱伝達，投影面積率，人体，熱的快適性，不均一温熱環境

1. INTRODUCTION

There are many situations where the evaluation of asymmetric thermal radiation environment is required. For example, environments in buildings near cold windows in winter, room environments controlled by heated or cooled panel systems, environments in large spaces like atria which have large temperature differences between floor and ceilings in addition to many cold/hot windows, and so on. In these highly asymmetric environments, radiation analysis is required not only for the whole body but also for individual body parts.

There is a strong need for a radiation analysis model at the body-part level, and for empirical data for the model (Stolwijk[1], 1971, Tanabe[2], 1998 etc.). The completion of such a model partly depends on new radiation analysis and empirical data describing each part of the human body.

There are many studies on evaluation of thermal comfort and heat transfer at the body-part level.[3)~10)] Also there are many studies on projected area for human body.[11)~15)] However there is no study which fully describes all the projected area factors at the body-part level for all the directions around the human body so that all the angle factors between any planes and each part can be estimated. This paper describes measurements of projected area factors for each part of the body so that radiation exchange between any surrounding plane and human body part under some assumptions or the effect of solar radiation on human body part can be calculated. We first describe ways to calculate angle factors, effective radiation area, radiative heat transfer coefficient, and mean radiant temperature for each segment of the human body under some conditions. Then we present measured distribution of projected area factors for 16 body segments. And effective radiation areas, effective radiation area factors, and angle factors are calculated and compared with other studies.

2. DESCRIPTION OF THREMAL RADIATION

Fanger[15] (1970) measured all the projected area factors of a whole human body as seen from all directions, using photographs taken from 7m away and calculated angle factors between a whole body and rectangular surfaces. Steinman[16] also calculated angle factors between a whole body and inclined walls using those data. Fanger's data are very useful because no matter what the distance is, angle factors can be calculated based on the projected area factor distribution. Horikoshi[17),18)]et al. (1978, 1988) and Tsuchikawa[19] et al. (1988) directly measured angle factors between rectangular planes and the human body using a special fisheye lens in the short distances. However those

* Taisei Corporation, M. Eng.　大成建設㈱　工修
** Prof., Center for Environmental Design Research, Univ. of California, Ph. D.
*** Center for Environmental Design Research, Univ. of California, M. Eng.
**** National Institute of Bioscience and Human-Technology, Ph. D.　生命工学工業技術研究所　Ph. D.
***** Prof., Dept. of Energy and Environmental Engineering, Interdisciplinary Graduate School of Engineering Sciences, Kyushu University, Dr. Eng.　九州大学大学院総合理工学府環境エネルギー工学専攻　工博

data can be used only for a whole human body.

Recently Tsuchikawa[20] et al. (1991) measured angle factors between rectangular planes and 4 parts of the human body (head, arms, trunk, and legs), using a fisheye lens from distances of 1 to 2.5 meters. However their angle factor diagrams can be used only in those distances.

In this study we took Fanger's approach to estimate the angle factors for each body part because angle factors can be calculated no matter what the distance is.

(1) Angle factor between a body part and a plane

Consider a man and a plane in the surroundings with surface area A_2. Consider one of the body parts with surface area A_1 and a differential element dA_2 out of the plane. Imagine the connecting line from the center of the body part to the center of dA_2. When the polar angle at dA_2 is θ_2 we can consider the angle factor between A_1 and $\cos\theta_2 dA_2$. According to the reciprocity theorem (ASHRAE FUNDAMENTALS,[21] 1997),

$$A_1 \, dF_{1\text{-}\cos\theta 2dA2} = \cos\theta_2 \, dA_2 \, F_{\cos\theta 2dA2\text{-}1} \qquad (1)$$

Where,

θ_2:polar angle (angle of incidence) between the connecting line of the center of the two differential surfaces and the normal of differential surface dA_1

A_1: effective surface area of the targeted body part

A_2: surface area of the plane

dA_2: differential surface area of the plane

$dF_{1\text{-}\cos\theta 2dA2}$: angle factor from the body part A_1 to the differential surface $\cos\theta_2 dA_2$

$F_{\cos\theta 2dA2\text{-}1}$: angle factor from the differential surface $\cos\theta_2 dA_2$ to the body part A_1

If dA_2 is very small,

$$dF_{1\text{-}dA2} = dF_{1\text{-}\cos\theta 2dA2} \qquad (2)$$

Therefore, the angle factor between A_1 and A_2 would be

$$F_{1\text{-}A2} = \int_{A2} dF_{1\text{-}dA2} = \int_{A2} dF_{1\text{-}\cos\theta 2dA2} = \int_{A2} (F_{\cos\theta 2dA2\text{-}1}/A_1) \cos\theta_2 dA_2 \qquad (3)$$

If the distribution of $F_{\cos\theta 2dA2\text{-}1}/A_1$ is known, the angle factor from a body part A_1 to a surface A_2 can be determined through numerical integration (Eq. 3).

On the other hand, from the definition of angle factor (ASHRAE FUNDAMENTALS,[21] 1997),

$$F_{\cos\theta 2dA2\text{-}1} = \int_{A1} (\cos\theta_1 \cos\theta'_2 dA_1/\pi R^2) \qquad (4)$$

Where,

θ_1:polar angle on the surface A_1, θ'_2:polar angle on the surface $\cos\theta_2 dA_2$,

R: distance between dA_1 and $\cos\theta_2 dA_2$

If the size of the body part A_1 and the portion dA_2 is very small compared to the distance R, one can consider that $\cos\theta'_2 \fallingdotseq 1.0$. Then Eq. (4) can be written as,

$$F_{\cos\theta 2dA2\text{-}1} = \int_{A1} (\cos\theta_1 dA_1/\pi R^2) = A_p/\pi R^2 \qquad (5)$$

$$A_p = \int_{A1} (\cos\theta_1 dA_1) \qquad (6)$$

Where, A_p is the projected area of the body part on the half sphere with radius of R whose center is at the center of the area $\cos\theta_2 dA_2$. However, if the size of the body part A_1 and the portion dA_2 are very small compared to the distance R, A_p can be approximated as the projected area of the body part to the plane which comes in contact with that half sphere at the center of the body part.

Now, by substituting Eq. (6) to Eq. (3),

Table 1. Surface areas

Body Segment	Surface Area(m^2)
Back	0.128
Chest	0.138
Head	0.117
Left Arm	0.050
Left Foot	0.043
Left Hand	0.038
Left Leg	0.090
Left Upper Arm	0.076
Left Thigh	0.160
Right Arm	0.051
Right Foot	0.042
Right Hand	0.036
Right Leg	0.090
Right Upper Arm	0.073
Right Thigh	0.166
Pelvic Region	0.170
Whole Body	1.469

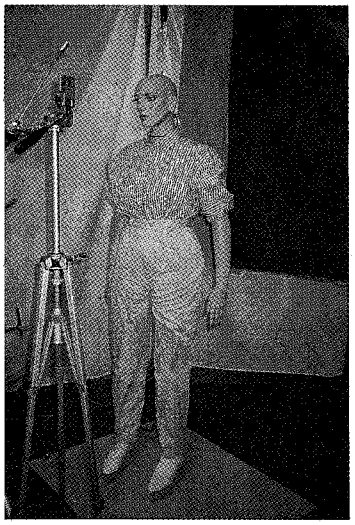

Figure 1. Thermal manikin

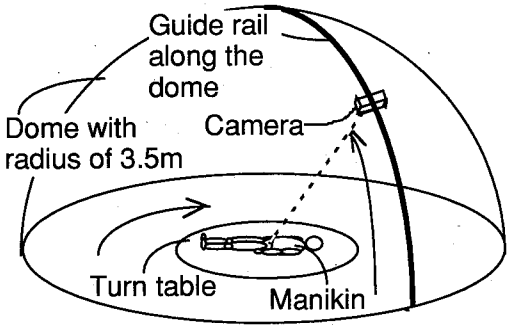

Figure 2. Experimental set-up for projected area measurement

$$F_{1\text{-}A2} = (1/\pi)\int_{A2} \{(f_P / R^2)\cos\theta_2\} dA_2 \quad (7)$$

$$f_P = (A_P / A_1) \quad (8)$$

Where,
f_P: projected area factor

Using Eq. (7), once fp distribution against all the directions is determined, any angle factor from a body part A_1 to any surface A_2 can be determined through numerical integration.

(2) Effective radiation area

Consider a large sphere with radius r instead of the plane A_2. Because $F_{1\text{-}A2}$ should be 1.0, the effective radiation area of the body part A_1 can be estimated from Eq.(9).

$$A_1 = (1/\pi)\int_{A2} \{(A_P / R_r^2)\cos\theta_r\} dA_r \quad (9)$$

$$f_{eff} = A_1 / A_m \quad (10)$$

Where,
dA_r: differential area on the sphere with radius r from which solid angles were measured
R_r: the distance between targeted part A_1 and dA_r
θ_r: polar angle on dA_r
f_{eff}: effective radiation area factor for the part A_1
A_m: actual surface area of the part A_1

Using (9), once fp distribution against all the directions is determined we can estimate the effective radiation area A_1. This effective radiation area estimation is needed only once for each posture of the human body. And by considering the body part as the whole human body, Eq. (7) through Eq. (10) can be used also for the whole human body.

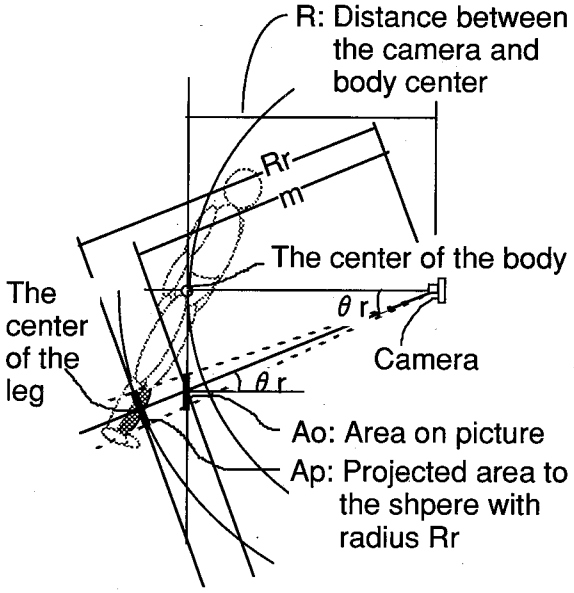

Figure 3. Estimation of Ap of a segment from pictures taken toward body center

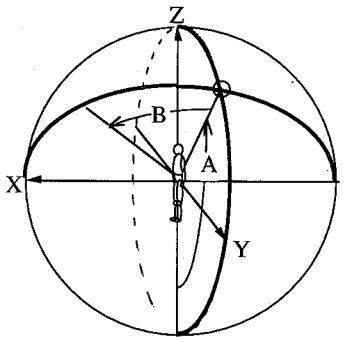

Figure 4. Coordinate system

(3) Radiation heat transfer coefficient

Strictly speaking, description of radiant heat transfer for each part of the human body has to include the radiation heat exchange between the body parts. However, under the conditions where the surface temperature difference between all the segments is very small and we can practically assume that heat transfer between the segments is negligible, the following formula (ASHRAE FUNDAMENTALS,[21] 1997) for whole human body can be used.

$$h_r = 4\,\varepsilon\,\sigma\, f_{eff}\{273.2 + (t_{cl} + t_r)/2\}^3 \quad (11)$$

Where,
h_r: radiation heat transfer coefficient for each segment, ε : emissivity for each segment,
σ :Stefan-Boltzmann constant, t_{cl}: surface temperature of the segment,
t_r: mean radiant temperature for each segment

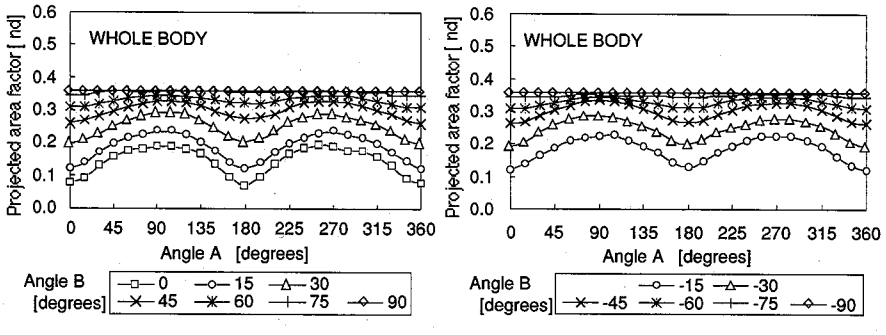

Figure 5. Projected area factor distribution for WHOLE BODY

Table 2. Coordinates of segments

Body Segment	Coordinates(m)		
	X	Y	Z
Back	-0.05	0.00	0.38
Chest	0.06	0.00	0.38
Head	0.08	0.00	0.69
Left Arm	-0.05	0.24	0.14
Left Foot	-0.05	0.11	-0.83
Left Hand	-0.02	0.27	-0.08
Left Leg	-0.05	0.12	-0.62
Left Upper Arm	-0.02	0.21	0.41
Left Thigh	0.00	0.12	-0.09
Right Arm	-0.07	-0.24	0.09
Right Foot	0.00	-0.11	-0.83
Right Hand	-0.03	-0.22	-0.12
Right Leg	-0.02	-0.11	-0.62
Right Upper Arm	-0.08	-0.21	0.41
Right Thigh	-0.02	-0.11	-0.11
Pelvic Region	0.00	0.00	0.11

(4) Mean radiant temperature for each segment

Strictly speaking, mean radiant temperature for each part of the human body has to include the effect of the radiation from the other body parts. However, under the conditions where the surface temperature difference between all the segments is very small and we can practically assume that heat transfer between the segments is negligible, the following formulae for the whole body (Olesen, [22] 1989) can be used also for each segment of the body.

$$\sigma (t_{ri}+273.2)^4=B_1 F_{i-1}+ B_2 F_{i-2}+ \ldots \quad + B_n F_{i-n} \qquad (12)$$

and

$$\Sigma F_{i-n} \quad =1 \qquad (13)$$

Where,

t_{ri}: mean radiant temperature for the segment named i, B_n: radiosity of surface n, F_{i-n}: angle factors between a segment i and surface n

Furthermore, assuming high emissivity for surrounding surfaces and relatively small temperature differences between the surfaces, the following formula for the whole body (Olesen, [22] 1989) can also be used for each segment of the body.

$$t_{ri}=t_1 F_{i-1}+ t_2 F_{i-2}+ \ldots \quad + t_n F_{i-n} \qquad (14)$$

Where,

t_n: temperature of surface n

In field measurement of mean radiant temperature, plane radiant temperature in 6 directions is sometimes used to estimate mean radiant temperature. It would be very convenient if we can estimate that for each part from plane radiant temperature in 6 directions as well. Olesen[22] (1989) suggested that mean radiant temperature for whole human body might be approximately calculated from the plane radiant temperature in six directions (up, down, left, right, front, and back) and weighted according to projected area factors of a person in the same six directions. Although further detailed study concerning the accuracy of this approximation, this idea might be also applicable for each part of the body, noting that any directions cannot be treated as symmetry.

Table 3. Comparison of effective radiation area factors for whole human body

	Present Study	Fanger et al. [15]	Tsuchikawa et al. [19]	Tsuchikawa et al. [20]	Ozeki et al. [5]	Miyazaki et al. [7]
Height	1.60	1.72	1.63	1.68	1.75	1.71
Surface Area	1.47	1.74*	1.51*	1.80*	1.72	1.58
Effective Radiation Area	1.24	1.26	1.22	1.44	1.28	1.32
Effective Radiation Area Factor	0.85	0.73	0.81	0.80	0.74	0.83

*DuBois Area

Table 4. Comparison of effective radiation areas

Body Segment	Effective Radiation Area(m^2)	Body Segment	Effective Radiation Area (m^2)		
	Present Study		Present Study	Tsuchikawa et al. [20]	Ozeki et al. [5]
Back	0.115	Head	0.11 9%	0.17 12%	0.12 9%
Chest	0.122				
Head	0.107				
Left Arm	0.041				
Left Foot	0.038	Body (Back+Chest +Pelvic Region)	0.38 31%	0.61 42%	0.52 41%
Left Hand	0.030				
Left Leg	0.084				
Left Upper Arm	0.063				
Left Thigh	0.137	Arms (Arms+Upper Arms +Hands)	0.27 22%	0.25 17%	0.26 20%
Right Arm	0.040				
Right Foot	0.039				
Right Hand	0.028				
Right Leg	0.080	Legs (Feet+Legs +Thighs)	0.52 42%	0.47 33%	0.38 30%
Right Upper Arm	0.066				
Right Thigh	0.140				
Pelvic Region	0.146				
Total	1.276		1.28 103%	1.50 104%	- -
Whole Body	1.242		1.24 100%	1.44 100%	1.28 100%
Surface Area			1.47	1.80*	1.72

*DuBois Area

Table 5. Effective radiation area factors

Body Segment	Effective Area Factor
Back	0.90
Chest	0.88
Head	0.91
Left Arm	0.83
Left Foot	0.87
Left Hand	0.80
Left Leg	0.93
Left Upper Arm	0.82
Left Thigh	0.86
Right Arm	0.78
Right Foot	0.91
Right Hand	0.78
Right Leg	0.89
Right Upper Arm	0.90
Right Thigh	0.85
Pelvic Region	0.86
Whole Body	0.85

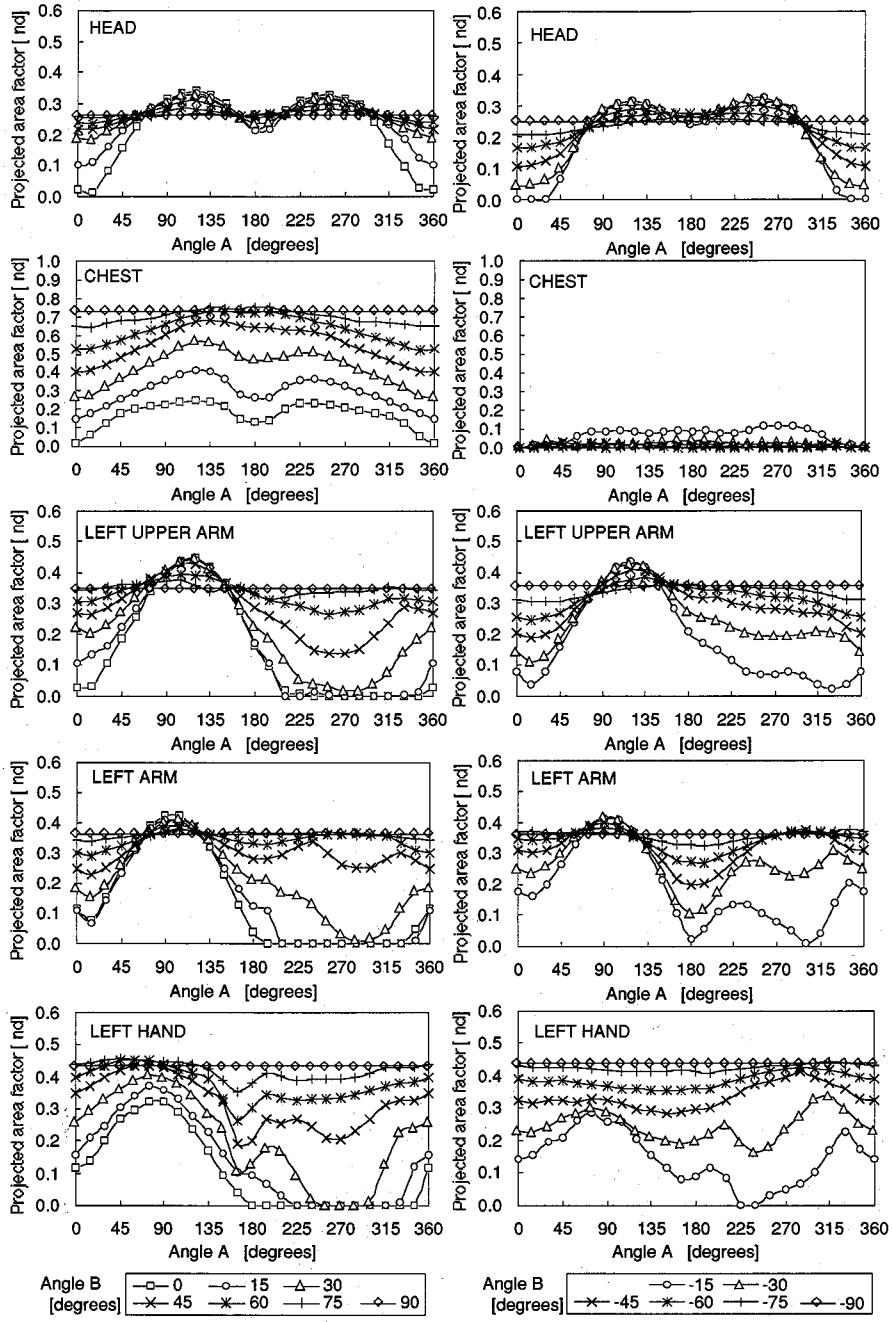

Figure 6-1. Projected area factor distribution for each part

$$t_{ri}=(f_p[up].t_{pr}[up]+f_p[down].t_{pr}[down]+ f_p[right].t_{pr}[right]+f_p[left].t_{pr}[left]+ f_p[front].t_{pr}[front]+f_p[back].t_{pr}[back])/ (f_p[up]+f_p[down]+f_p[right]+ f_p[left]+f_p[front]+ f_p[back]) \quad (15)$$

$f_p[\ ]$: projected area for each of 6 directions

$t_{pr}[\ ]$: plane radiant temperature from each of the 6 directions

3. MEASUREMENT OF PROJECTED AREA FACTORS

(1) Thermal Manikin

A segmented thermal manikin (Tanabe, [23] 1994) was used for the measurement of projected area of the human body segments. This manikin, of female shape, is one of several developed to evaluate asymmetric thermal environment by measuring the heat loss at each part of the body. Fig.1 shows a picture of the thermal manikin. The 16 body segments and their respective surface areas are listed in Table 1. The manikin was chosen for the radiation study based on the following considerations:

a. The surface area of each segment is clearly defined.
b. Combination of heat loss measurement and this radiation study enables us to separate radiative and convective heat transfer[3),4)].
c. There is almost no limitation concerning measurement procedure.

(2) Measurement procedure

A sky simulator dome of radius 3.5m was used for this radiation study. The facility has a guide rail running longitudinally to the zenith. In normal use, a light representing the sun travels up

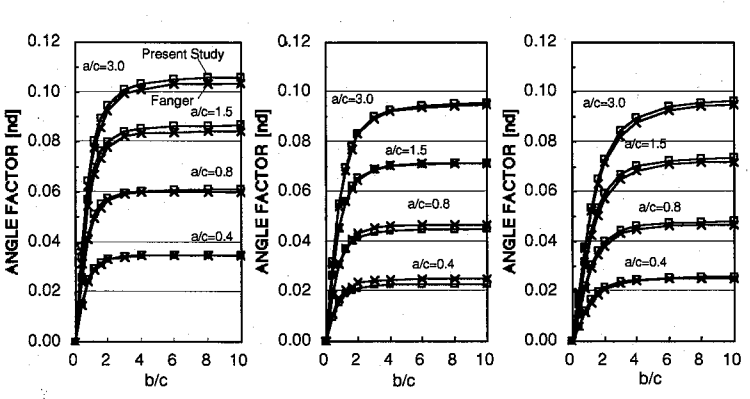

Figure 7 Comparison of angle factor with Fanger's results (left: front walls, middle: side walls, right: ceilings)

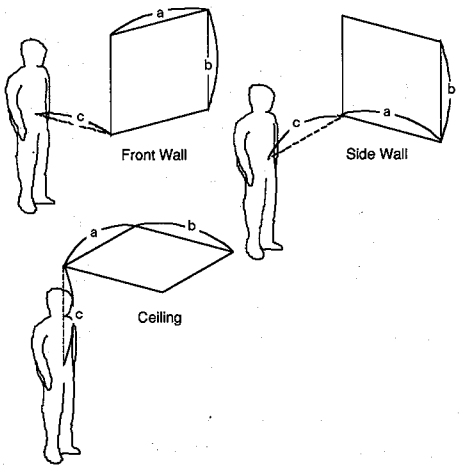

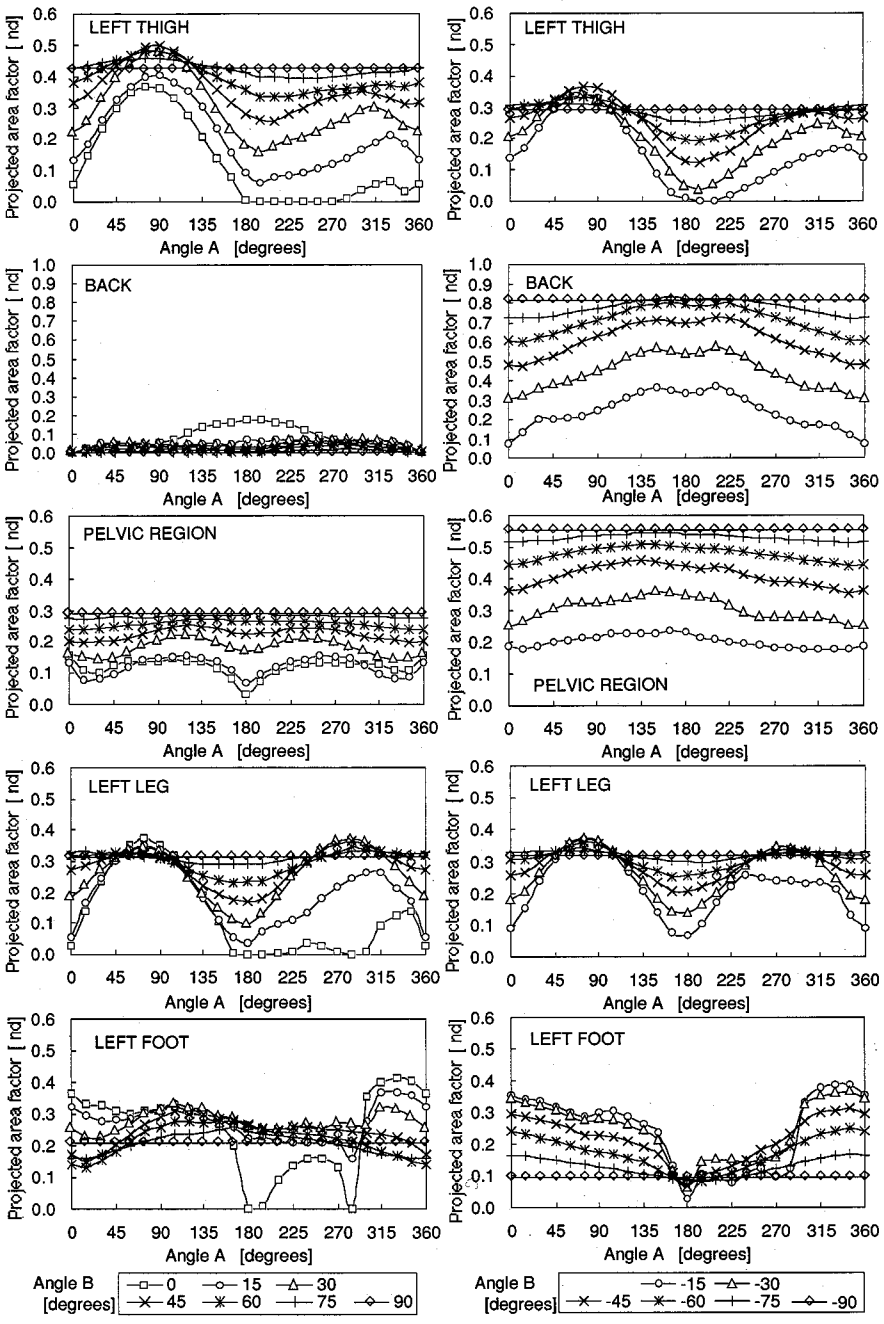

Figure 6-2. Projected area factor distribution for each part

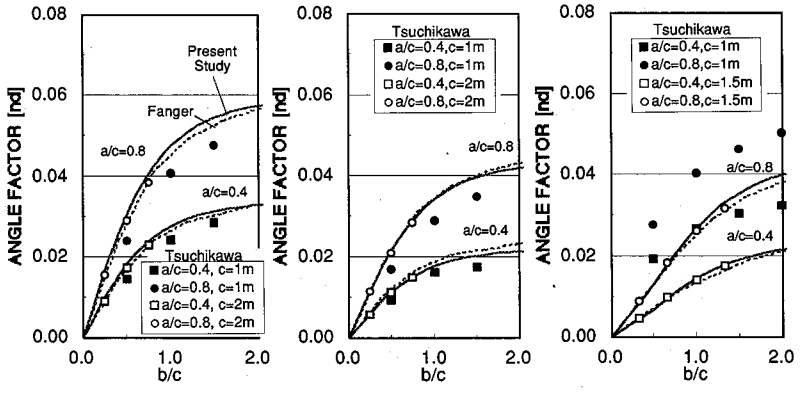

Figure 8 Comparison of angle f actor in short distances
(left: front walls, middle: side walls, right: ceilings)

and down this rail on a motorized carriage. A turntable at the base of the half sphere allows the sun's azimuthal movement to be simulated. By setting a camera instead of the light bulb on the carriage and laying the manikin on the turntable, one can easily take pictures from all directions. Fig.2 is the experimental set-up for measuring the manikin's projected areas. First the manikin was set on her back on the turntable and rotated in the horizontal plane. Pictures were taken with a 35mm camera with a 50mm lens. For 0, 15, 30, 45 degrees vertical angle, pictures were taken at every 15 degrees in horizontal angle. For 60 and 75 degrees vertical, pictures were taken every 30 degrees in horizontal angle. One picture was taken at 90 degrees. After recording the manikin on her back, the manikin was turned over and set face-down. Then the above-mentioned procedure was repeated. The center of the pelvic region was set at the center of the dome throughout the experiment. The center of the body was 0.86m above the floor for the standing manikin.

In addition, pictures of a ball with radius of 239mm were taken in order to determine the conversion ratio from the negative area (measured in number of pixels) to the actual area in square meters.

(3) Estimation of projected area

All the films were developed and the negatives were used to analyze projected areas. The negatives were digitized at 1000 dots per inch resolution. The number of pixels was counted by using computer software (SigmaScan 2.00) for image measurement.

The conversion ratio from pixels to actual projected area was estimated by dividing the known projected area of the ball by the number of the pixels in its photograph. This conversion ratio was used for all the picture analyses. The areas estimated in the above manner correspond to the area on the plane normal to the direction of the camera at the distance of 3.5m. Thus the areas further away have to be converted to the required projected areas at the position of each segment. For this purpose the coordinates for each segment of the body were also measured from the pictures taken from the top of the dome and in the horizontal plane. Fig.3 shows the relationship between projected area Ap and the area estimated from counting the number of pixels. Ap can be

estimated as follows.

$$A_p = A_0 (m / R_r)^2 \cos\theta_r \qquad (16)$$

Where,
A_0: the area on the plane normal to the direction of the camera at the distance of 3.5m, m: the distance between the A_0 and the camera,
R_r: the distance between targeted part and the camera, θ_r: polar angle on dA_0

4. RESULTS AND DISCUSSION

Fig. 4 shows the orthogonal coordinate system for the segment of the body and the spherical coordinate system for projected area distribution. The measured locations for each part of the body are shown in Table 2, in the orthogonal coordinate system. The conversion ratio of actual area to the number of pixels is 0.0228 square centimeters per pixel. Projected area factors are presented in the spherical coordinate system. Results for the manikin on her back are presented as the results for the front side of the human body, and those for the manikin on her face are presented as the results for the back side of the human body.

(1) Effective radiation area and effective radiation area factor

First the projected area distributions were acquired, then numerical integration based on the Eq. (9) was carried out. The calculated effective radiation areas and the effective radiation area factors for the whole body are listed in Table 3, compared with the results from other studies. The total body effective radiation area factor in this study is 0.85 and lager than the other studies. This may be due to slight difference of standing posture, i.e., the posture of the manikin in this study may be slightly more open than the others. The results for each part of the body are listed in Table 4, compared with Tsuchikawa's and Ozeki's results. When comparing in terms of head, body, arms, and legs based on Tsuchikawa's definition, the ratios of each part to the total are pretty consistent with the other two studies. The differences of about 10% in body and legs may be due to the difference of the line dividing the body and legs. The largest effective radiation areas, in order, are the pelvic region, thighs, chest, and back. The order of the actual surface areas is the same. The effective radiation area factors based on Eq. (10) are also listed in Table 5. The effective radiation area factors at hands and arms are a little less than other segments. This can be explained by blocking effect of the trunk that exists along those segments.

(2) Projected area distribution

Eq. (8) gives us the projected area factors, and these enable us to calculate angle factors from each part of the body to any plane. Fig. 5 shows the results of the distribution of the projected area factor for the whole human body. Concerning whole-body results, the distribution is symmetrical between A <180° and A>180° as might be expected. Symmetry can also be seen between the front side and back side as expected. The maximum value of fp is 0.36 for B=90° and -90° and minimum value of fp is 0.07 for (A, B)=(180°, 0°). Because our coordinate system is different from Fanger's, all the results cannot be directly compared. However, these results are almost consistent with Fanger's results, i.e., maximum fp is 0.35 and minimum fp is 0.08 at the same angles.

Fig. 6-1 to 6-2 show the results of the distribution of projected area factors for each segment. For example, in the left arm we can understand that the left arm can not be seen from her front side because it is almost perfectly blocked by other body parts when A is 225° to 315° and B is less than or equals 15°. When comparing between the front side and back side, it is easy to understand that for the back and chest distributions look as if they were changing places between front side and back side. However, any segment including limb parts cannot have the symmetrical distribution between the front side and back side as appeared for the whole body. This can be explained in that some of them are blocked by a different segment when seen from the front side versus back side. Some of them also have different shapes from the front and back because of the slope of the lines dividing the segments of the whole body.

(3) Angle factor

Based on Eq. (7), angle factors between the whole body and a rectangle in front of the human body were calculated for a comparison with Fanger's and Tsuchikawa's results. Fig. 7 shows the results for the whole body with Fanger's data. The difference was within 10%. In considering the difference of height of his subjects versus the manikin (172/160 centimeters), it can be said the results are in very good agreement. Fig. 8 shows the comparison with Tsuchikawa's results for short distances. For c=2m in front and side walls, also for c=1.5m in ceilings, In considering the difference of height of their subject and our manikin (167.7/160 centimeters), it can be said the results are in very good agreement. However, for c=1m, our results and Fanger's are significantly different from Tsuchikawa's results in many cases. These results suggest that our data can be used for walls at 2m or more distant or ceilings 1.5m or more distant and for short distances such as 1m, Tsuchikawa's results should be used.

5. SUMMARY

We provided a description of important elements in radiative heat transfer for each part of the body. In addition we actually measured the projected area factors for each part of the body by using a standing thermal manikin. Angle factors were calculated from these measured data and compared with other studies. The comparison generally showed good agreement and demonstrated that our data can be used for distant walls or ceilings as well as Fanger's data. The projected area factors for each body part measured in this study can be used in many ways to investigate radiation heat transfer to and from each part of the human body.

References

1) J. A. J. Stolwijk: A mathematical model of physiological regulation in man, NASA, CR-1855, 1971.

2) S. Tanabe, S. Horikawa, M. Kin, H. Tsutumi: Comparison of physiological values calculated by a 65 node thermoregulation-model with subjective experiments, Proceeding of SHASE, pp. 989-992, 1998.

3) R. deDear, E. Arens, H. Zhang, M. Oguro: Convective and radiative heat transfer coefficients for individual human body segments, International Journal of Bio meteorology, Vol. 40, No. 3, pp. 141-156, 1997.

4) M. Ichihara, M. Saitou, M. Nishimura, S. Tanabe: Measurement of convective and radiative heat transfer coefficients of standing and sitting human body by using a thermal manikin, Journal of Architectural Planning and Environmental Engineering, AIJ, No. 501, pp.45～51, 1997.

5) Y. Ozeki, M. Konishi, C. Narita, Y. Kurazumi, S. Tanabe: Angle factors between human body and rectangular planes calculated by a numerical model, Journal of Architectural Planning and Environmental Engineering, AIJ, No. 522, pp. 15-22, 1999.

6) K. Suzuki, N. Kakitsuba, Development of a human body model based on the human body area and the configuration factors, Journal of Architectural Planning and Environmental Engineering, AIJ, No. 515, pp. 49-55, 1999.

7) Y. Miyazaki, M. Saito, Y. Seshimo, A study on evaluation of Non-uniform thermal environments by human body model Part1, Journal of Human and Living Environment, No. 1, pp. 92-100, 1995.

8) J. Ishii, T. Horikoshi, S. Watanabe, K. Suzuki, Y. C. Zhi, Experimental estimation of natural convective heat transfer coefficients for the human body and its segments, Journal of Architectural Planning and Environmental Engineering, AIJ, No. 530, pp. 31-37, 2000.

9) T. Horikoshi, T. Tsuchikawa, Y. Kurazumi, K. Hirayama, Y. Kobayashi, Indication of asymmetric and uneven thermal radiation environment related to thermal comfort and discomfort, Journal of Architectural Planning and Environmental Engineering, AIJ, No. 413, pp. 21-28, 1990.

10) T. Miyanaga, W. Urabe, Y. Nakano, A. Hoyano, Study on improvement of living thermal environment by radiant cooling part2, Journal of Architectural Planning and Environmental Engineering, AIJ, No. 526, pp. 51-58, 1999.

11) W. Underwood, The solar radiation area of man, Ergonomics 9(2), pp. 155-168, 1966.

12) Y. Ozeki, M. Konishi, C. Narita, Y. Kurazumi, S. Tanabe: Evaluation on effective radiation area of human body calculated by a numerical simulation, Journal of Architectural Planning and Environmental Engineering, AIJ, No. 525, pp. 45-51, 1999.

13) S. Miyamoto, T. Horikoshi, Y. Hirokawa, Projected area factors of the human body at standing posture under different clothing conditions, Journal of Architectural Planning and Environmental Engineering, AIJ, No. 513, pp. 47-52, 1998.

14) A. Tomita, S. Miyamoto, T. Horikoshi, The influence of clothing fit on the projected area of the human body at standing posture, Journal of Architectural Planning and Environmental Engineering, AIJ, No. 518, pp. 7-12, 1999.

15) P.O. Fanger, O. Angelius, P. Kjerulf-Jensen: Radiation data for the human body, ASHRAE Transactions, Vol. 76, pp.338-373, 1970.

16) M. Steinman, L. N. Kalisperis, L. H. Summers: Angle factor determination from a person to inclined surfaces, Vol. 76, pp.1809-1823, 1988.

17) T. Horikoshi, H. Miyahara, Y. Kobayashi, Configuration factors between the human body and rectangular planes and the effective radiation area of the human body Part1, Transaction of AIJ, No. 268, pp. 109-119, 1978.

18) T. Horikoshi, Y. Kobayashi, Configuration factors between the human body and rectangular planes and the effective radiation area of the human body Part2, Transaction of AIJ, No. 322, pp. 92-99, 1982.

19) T. Tsuchikawa, T. Horikoshi, E. Miwa, Y. Kurazumi, K. Hirayama, Y. Kobayashi: The effective radiation area of the human body and configuration factors between the human body and rectangular planes measured by photographic method Part1, Journal of Architectural Planning and Environmental Engineering, AIJ, No. 388, pp. 48-45, 1988.

20) T. Tsuchikawa, T. Horikoshi, E. Kondo, Y. Kurazumi, K. Hirayama, Y. Kobayashi: The effective radiation area of the human body and configuration factors between the human body and rectangular planes measured by photographic method Part2, Journal of Architectural Planning and Environmental Engineering, AIJ, No. 428, pp. 67-75, 1991.

21) ASHRAE, ASHRAE HANDBOOK FUNDAMENTALS, 1997.

22) B. W. Olesen, J. Rosendahl, L. N. Kalisperis, L.H. Summers, M. Steinman: Methods for measuring and evaluation the thermal radiation in a room, ASHRAE Transactions, Vol. 95, Part1, 1989.

23) S. Tanabe, E. Arens, F. Bauman, H. Zhang, M, T. Madsen: Evaluating thermal environments using a thermal manikin with controlled surface skin temperature, ASHRAE Transactions, Vol. 100, 1994.

和文要約

1. はじめに

不均一な放射環境の評価を求められる状況は多い。例えば、冬季の建物内の窓近傍、放射パネルにより調整された室内、アトリウムなど、床と天井に大きな温度差が発生した大空間などである。このように大きな不均一放射が生じている状況では人体を全体として捕らえるだけでなく、部位毎に捕らえて評価していくことが必要と考えられる。

本報告は、 Fanger と同様の考え方を用いて、人体の 16 部位を対象として、方向別の投影面積分布を計測により求めると共に、有効放射面積、有効放射面積率、形態係数を算出し、その妥当性を検証したものである。

2. 放射熱交換の定式化

人体各部位と任意の平面の間の形態係数は最終的に（7）式、（8）式で表され、投影面積率の分布が解れば、形態係数を求めることができることになる。

人体各部の有効放射面積率は最終的に（9）式、（10）式で表され、投影面積の分布が解れば、有効放射面積率を求めることができることになる。

人体各部の放射熱伝達係数は（11）式で表され、有効放射面積率が解れば、放射熱伝達係数を求めることができる。

人体各部の平均放射温度は（12）式や（14）式で表され、形態係数が解れば、平均放射温度を求めることができる。また、実測等では 6 方位の平面放射温度から（15）式により概算することも可能と考えられる。

3. 計測方法

（1）サーマルマネキン

計測は、表面積が正確に把握出来ること、測定方法の制限が少ないこと、対流熱伝達率と放射熱伝達率の正確な分割の可能性を考慮し、人体を模擬したサーマルマネキンを対象として行った。対象としたマネキンは皮膚温度可変型のサーマルマネキンで、主に室内の不均一温熱環境の評価用として開発されたものである。図-1 にサーマルマネキンを示す。部位の分割数は 16 であり、表面積は表-1 のようになっている。

（2）計測方法

図-2 に計測方法の概念図を示す。ドームの半径は約 3.5mである。マネキンをドームの中心にあるターンテーブルに仰向けあるいはうつむけに設置し、カメラ（50mm 普通レンズ）をドーム屋根に沿って移動する台に取り付けた。カメラは屋根に沿って上下し、遠隔で撮影が行えるようになっている。この装置を用いて、人体に対して、左右上下を含めた全角度からの撮影を行った。上下方向は 0 °、15 °、30 °、45 °、60 °、75 °、90 ° とし、90 ° を除き、それぞれに角度に対して水平方向 360 ° の撮影を行っている。水平方向の角度は、上下方向の角度 0 °、15 °、30 °、45 ° では、15 ° 毎、上下方向の角度 60 °、75 ° では 30 ° 毎とし、上下方向 90 ° では 1 回の撮影とした。

（3）投影面積率の算出方法

ネガから 1000ＤＰＩの解像度でパソコンに画像情報として取込み、ピクセル数を計測することにより、面積を算出した。ピクセル数から面積への換算比は、別途、直径が既知の球状の物体をドームの中心において撮影を行い、画像のピクセル数と実際の投影面積から求めた。さらに、中心からずれた部位に関しては図-3 の幾何学的関係から（16）式に基づき、部位毎、角度毎に補正を行った。

4. 計測結果

（1）有効放射面積および有効放射面積率

全身の有効放射面積率（表-3）は 0.85 となり、他の研究と比較してやや大きな値となった。これは、本研究の立位が他研究に比べ足や腕の開き大きいことによると思われる。また、部位毎の有効放射面積（表-4）は土川等や尾関等の結果と対応した結果が得られた。足と胴体で 10%程度差があるのは足と胴体の分割位置が異なるためと考えられる。手、腕の有効放射面積率は他の部位よりやや小さい。これは、胴の部分に沿っているため、胴に遮られる割合が大きいためと考えられる。

（2）投影面積分布

全身の投影面積率分布を図-5 に示す。全身でみると、Ｂ＝90 °、-90 ° において、最大 0.36、Ａ=180 °、Ｂ＝0 ° で最小値 0.07 となり、Fanger の結果とほぼ一致している。人体各部の投影面積率分布を図-6-1、6-2 に示す。全身の場合と異なり、遮へいする人体の部位が正面と背面で異なり、また、各部を分割する線の見え方も異なるので、いずれの部位も正面と背面で対象とはならない。

（3）形態係数

全身について、正面・側面・天井にある平板との形態係数を算出し、Fanger 結果と比較した（図-7）。その結果、その差は10%以内であり、体型の違いを考慮すれば、よく一致している。また、全身について、至近距離（1m～2.5m）で測定された土川等のデータとの比較を行った（図-8）。その結果、正面・側面の平板に対して 2m、天井にある平板に対して 1.5mのケースではほぼ一致した結果が得られ、それ以上離れた壁に対して適用可能であることが示された。一方、1mのケースではかなり差がみられ、１ｍという至近距離では土川らのデータを使う必要があることが示された。

5.まとめ

部位別の放射解析に必要な要素として、形態係数、有効放射面積率、放射熱伝達係数、平均放射温度の定式化を行うとともに、マネキンを対象として、部位別の投影面積率の全方位分布を計測した。また、有効放射面積、有効放射面積率、形態係数を算出し、他の研究と比較を行った。1ｍという至近距離での形態係数を除き、ほぼ対応する結果が得られ、ある程度離れた壁や天井に対しては十分適用可能であることが示された。

（2000年９月８日原稿受理，2001年４月18日採用決定）